This full text paper was peer-reviewed at the direction of IEEE Instrumentation and Measurement Society prior to the acceptance and publication.

Optimized Design of the MEMS-Based Three-Axis Thermal Accelerometer for Its Better Performance in a Wide Measurement Range

A.I. Ovodov
MEMSEC R&D Center
National Research University of Electronic Technology (MIET)
Moscow, Zelenograd, Russia
ovodov@ntc-nmst.ru

G.D. Demin
MEMSEC R&D Center
National Research University of Electronic Technology (MIET)
Moscow,Zelenograd, Russia
gddemin@gmail.com

N.A. Djuzhev
MEMSEC R&D Center
National Research University of Electronic Technology (MIET)
Moscow,Zelenograd, Russia
djuzhev@ntc-nmst.ru

M.A. Makhiboroda
MEMSEC R&D Center
National Research University of Electronic Technology (MIET)
Moscow,Zelenograd, Russia
m.makhiboroda@gmail.com

***Abstract*— A new design of the three-axis thermal accelerometer with a set of temperature sensing elements (thermistors) in the direction of each axis located on a thin-film SiO2 membrane is proposed. Finite-element study of the accelerometer with the selected design shows that the temperature difference between the symmetrically placed thermistors linearly increases with acceleration in the range from 1g to 10g. At the same time, with increasing their distance from the central heater the sensitivity of thermistors reaches a maximum value, and then gradually drops to zero near the edge of the membrane. It was also found that in order to achieve the maximum thermal sensitivity when detecting acceleration in the lateral direction, thermistors should be asymmetrically placed relative to the heater along the corresponding axis, and the asymmetry of their optimal location on the membrane increases with acceleration. The results obtained can be used to improve the design of MEMS (Micro-Electro-Mechanical-System) accelerometers based on thermal effects.**

Keywords—three-axis thermal accelerometer, MEMS, thermoresistive sensors, fluid, silicon technology

I. INTRODUCTION

Nowadays, sensorics plays an important role in the development of mobile phones, high-tech gadgets, smart health monitoring devices (control of body temperature, blood pressure, pulse rate, etc.), as well as for the integration of intelligent electronic systems in cars, space satellites and unmanned aerial vehicles (drones) for civilian applications [1]. Small-scale MEMS accelerometers, which can provide the user with information about the static (gravitational) or dynamic acceleration, like shock or vibration, take a leading place in this direction. For example, they become indispensable for preventing the crash of portable electronic devices (hard drives, handbooks) after their free fall, structural health monitoring of buildings, bridges and predicting possible causes of equipment failure, improving human safety in road traffic accidents (in anti-lock braking systems, airbags) and to detect the angle of rotation and orientation in digital cameras, drones, tablets. There are various types of MEMS accelerometers whose design involves the use of proof mass to determine the value of acceleration — field-emission [2], piezoresistive [3] and capacitive [4] MEMS accelerometers. The main disadvantage of these kinds of accelerometer is the low resistance to shocks, in particular, when working in extreme conditions, which is caused by the mechanical mobility of the solid proof mass, which leads to irreversible destruction of fragile parts of the accelerometer design. In contrast, the principle of operation of thermal MEMS accelerometers is based on the displacement of the hot fluid on the top of the heater within the cavity under the action of acceleration, which does not require the use of moving mechanical objects (Figure 1).

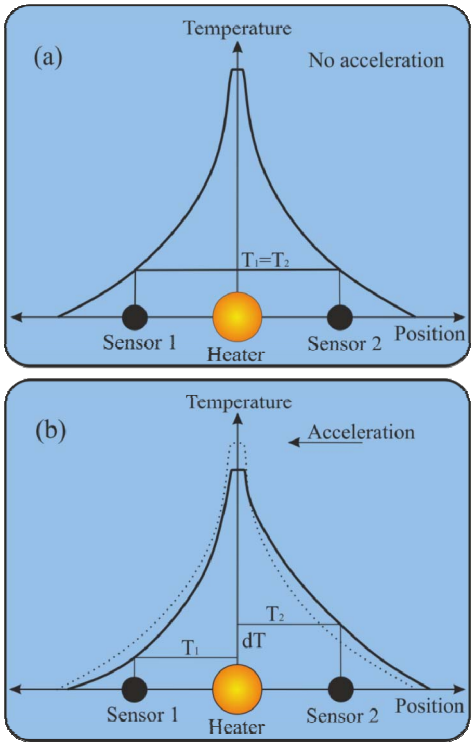

Fig. 1. The principle of the thermal accelerometer. (a) In the case of zero acceleration, there is thermal equilibrium between the sensing elements Sensor 1 and Sensor 2 and no temperature difference is observed, i.e. $T_1=T_2$. (b) The applied acceleration shifts hot fluid bubble in the direction opposite to its action. Thus, the temperature difference $dT=T_2-T_1$ due to the shift of the temperature profile is detected by sensing elements Sensor 1 and Sensor 2 (thermal resistors or thermopiles) located on both sides of the heater.

978-1-5386-7713-1/19/$31.00 ©2019 IEEE

As shown in Figure 1, the shift of a hot fluid bubble located above the heat source opposite to the direction of acceleration vector due to free-convection heat transfer leads to the difference in temperature of sensing elements (Sensor 1 and Sensor 2) placed on both sides of the heater along the given direction of acceleration. This, in turn, causes the appearance of a non-zero voltage signal, taken from the sensing elements, which is determined by the thermoresistive [5] or thermoelectric effect [6]. To detect X-axis or Y-axis acceleration, as a rule, symmetric sensing elements are placed in the plane of accelerometer along the respective axes [7, 8]. Previously, a large number of studies were carried out to optimize the design of a two-axis thermal accelerometer [9, 10], mainly aimed at increasing the sensitivity and expanding the operating frequency range of the sensor, which are complementary tasks. These tasks can be solved by selecting the appropriate gases, choosing the optimal shape of the heater, parameters of the conductive substrate, etc.

However, despite notable progress in this area, there is still no definitive answer to the question of what is the best way to build a three-axis accelerometer design, where the hot bubble also shifts in a direction perpendicular to the plane of the thin-film membrane, on which the heating element is usually located. The arrangement of thermistors (or thermocouples) along the out-of-plane axis complicates the technological process of creating an accelerometer, as well as its mass and compactness. Previously, the idea was proposed to locate all sensing elements in the plane of the heating resistor on the membrane, which can be realized by creating an asymmetric cavity along the OZ axis, which makes it possible to laterally change the shape of the shifted heat bubble depending on the direction of out-of-plane acceleration and, therefore, detection of this acceleration component [11-14]. However, the out-of-plane sensitivity of the thermal accelerometer with the design proposed in these works is orders of magnitude less than the sensitivity in the lateral direction [15]. At the same time, when adding both in-plane and out-of-plane acceleration to the thermal accelerometer leads to cross-axis sensitivity and the impossibility of unambiguously determining the correspondence between the temperature difference along a given axis and the related acceleration component [16]. Due to the above reasons, the search for the optimal design of a three-axis accelerometer is an urgent and important issue up to date.

II. Theory and Sensor Design

To optimize the operating parameters of the three-axis thermal accelerometer, the Comsol Multiphysics software package was used [17], on the basis of which the finite-element model of the three-axis thermal accelerometer design proposed in this work with a set of sensitive thermoresistive elements on a thin dielectric membrane was built.

A. Background

To calculate the change in temperature distribution of fluid under the action of acceleration, the following system of equations was used in the model of three-axis thermal accelerometer, based on the law of conservation of mass, momentum and energy:

$$\begin{cases} \dfrac{\partial \rho}{\partial t} + \nabla \cdot (\rho \mathbf{u}) = 0 \\ \rho\left(\dfrac{\partial \mathbf{u}}{\partial t} + \mathbf{u} \cdot \nabla \mathbf{u}\right) = -\nabla p + \nabla \cdot \boldsymbol{\tau} + \mathbf{F}_\mathrm{V} \\ \rho C_p\left(\dfrac{\partial T}{\partial t} + u \cdot \nabla T\right) = k\nabla^2 T \end{cases}, \quad (1)$$

where $\mathbf{u}$ is the flow velocity vector, p is the pressure, T is the temperature of the fluid flow, $\boldsymbol{\tau} = \mu\left(\nabla \mathbf{u} + (\nabla \mathbf{u})^T\right) - 2\mu(\nabla \cdot \mathbf{u})\mathbf{I}/3$ is the viscous stress tensor, $\mathbf{I}$ is the identity matrix, $\mathbf{F}_\mathrm{V} = -\rho \mathbf{a}$ is the volume force vector, $\mathbf{a} = \sum_{i=x,y,z} a_i \mathbf{e}_\mathbf{i}$ is the acceleration vector, a_i and $\mathbf{e}_\mathbf{i}$ are the acceleration and the unit vector along i-axis, ρ, μ, k, C_p are the density, dynamic viscosity, thermal conductivity and specific heat of the fluid, respectively. For the final description of the governing equations predicting the temperature distribution in a thermal accelerometer further we use the ideal gas law for the fluid density ρ which is valid in the case of compressible flow (when the Mach number is less than 0.3):

$$\rho = pM_f / RT, \quad (2)$$

where M_f is the molar mass of the gas, R is the universal gas constant. As the boundary conditions for the fluid flow, we assume that there is no slip condition ($\mathbf{u} = 0$) at the interface solid/fluid. This system of equations (1) and (2) was implemented in Comsol MultiPhysics by linking three different physical modules, describing the effect of Joule heating (module "Electric current"), heat dissipation (module "Heat transfer") and the convective heat transfer in the fluid under the applied acceleration (module "Laminar flow"). The interactions between these modules are schematically presented in Figure 2.

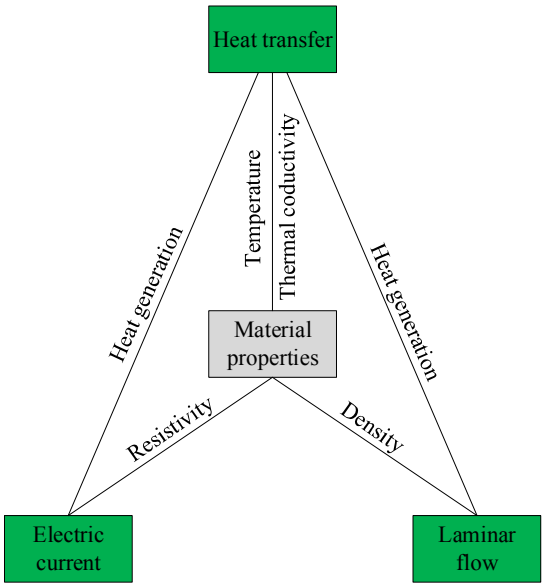

Fig. 2. Interactions between the modules of Comsol Multiphysics to describe the model of a thermal accelerometer.

The "Electric current" module is used to set the power supplied to the heater, on the basis of which the "Heat

transfer" module determines the amount of heat transferred to the fluid medium. In turn, the "Laminar flow" module determines the shift of the heat bubble and the corresponding change in the temperature profile, which according to formula (1) is associated with a change in the fluid density at non-zero acceleration.

B. Proposed Design of the Thermal Accelerometer

In this paper we propose the design of a three-axis thermal accelerometer, shown in Figure 3.

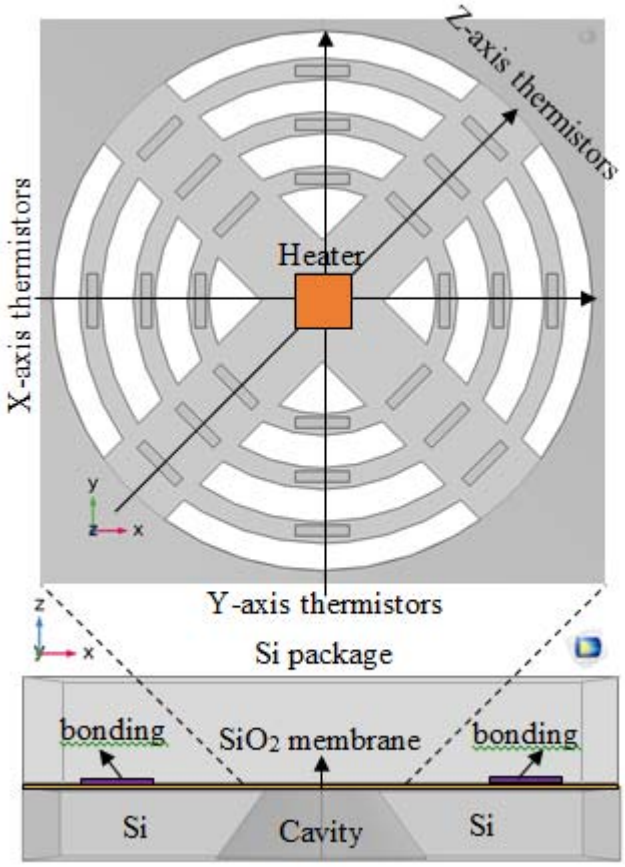

Fig. 3. The proposed design of the three-axis thermal accelerometer.

The heating central resistor (heater) and a set of sensing thermoresistive elements in the three directions of detection are located on a thin-film dielectric SiO_2 membrane in the cavity of the silicon substrate. The location of sensitive thermistors at different distances from the heater allows you to increase the overall sensitivity of the thermal accelerometer and set their optimal location during the simulation. Platinum with a high coefficient of thermal resistance equal to $3 \cdot 10^{-3}\ ^0C^{-1}$ according to our measurement results was chosen as the material for thermistors [18]. Also, as an alternative to thermistors, Al/Si* thermocouples can be used as sensing elements to improve measurement accuracy [19].

III. Simulation Results and Discussion

We consider the case when the acceleration along the axis OY (a_Y) is equal to 5g, along the axis OZ (a_Z) – g, and the acceleration a_X along the axis OX varies in the range from 1g to 10g. Figure 4 shows the temperature profile along the XOZ cross-section of the thermal accelerometer, the heating resistor of which is supplied with a power of 3.1 mW during the action of acceleration component $a_X = 5g$. As it follows from the figure, at this power, the maximum temperature T on the heater changes by 120 K from the initial room temperature T0 equal to 293.15 K. In this case, steps are visible on the temperature profile corresponding to the arrangement of the thermistors R_{-x1}, R_{-x2}, R_{-x3} on the left and R_{+x1}, R_{+x2}, R_{+x3} on the right in relation to the position of the heater along the axis OX.

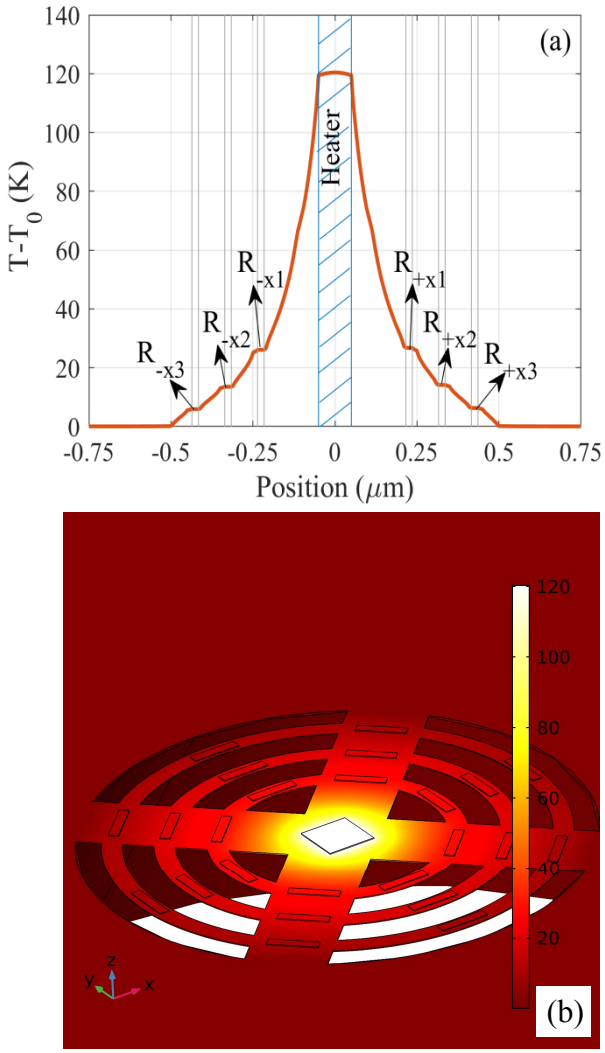

Fig. 4. (a) The temperature profile $T\text{-}T_0$ in the XOZ cross-section of the thermal accelerometer and (b) the temperature distribution (in K) along the membrane plane in the case, when the input heat power is equal to 3.1 mW, $a_Z = g$, $a_Y = 5g$ and $a_X = 5g$.

Figure 5 (a) shows the temperature change ΔT_{xy} along the line along the OX axis when the acceleration a_X varies from 1g to 10g with respect to the case when this acceleration component is zero, i.e. $a_X = 0g$. With increasing acceleration, the temperature of the right-side thermistors R_{+x1}, R_{+x2}, R_{+x3} increases, while the temperature of the left-side thermistors R_{-x1}, R_{-x2}, R_{-x3} drops, which is due to the shift of the hot fluid bubble in OX direction under the acceleration. In this case, the maximum temperature change is observed in the position of the thermistors corresponding to the distance from the heater equal to about 0.27 μm.

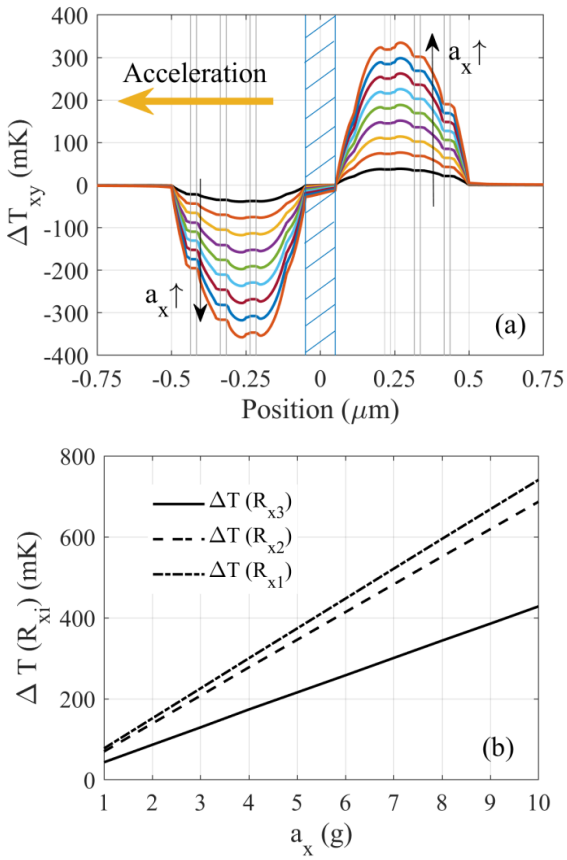

Fig. 5. (a) The temperature change $\Delta T_{xy} = \Delta T_{xy}(a_X) - \Delta T_{xy}(0g)$ along the axis OX, when the acceleration a_X varies from 1g to 10 g. (b) The temperature difference $\Delta T(R_{xi}) = \Delta T(R_{+xi}) - \Delta T(R_{-xi})$ at thermistors as a function of the acceleration component a_X, where $i = 1,2,3$, $a_Z = g$, $a_Y = 5g$, and the input heat power is equal to 3.1 mW.

At the same time, it is clear that the temperature change $\Delta T(R_{xi}) = \Delta T(R_{+xi}) - \Delta T(R_{-xi})$, where $i = 1,2,3$, is a linear function of acceleration and increases almost 8 times with increasing a_X from 1g to 10g, which is easily seen from Figure 5 (b). In turn, for the case of a change in acceleration a_Z in a similar range, such an effect of an increase in the temperature difference is not so noticeably observed (Figure 6).

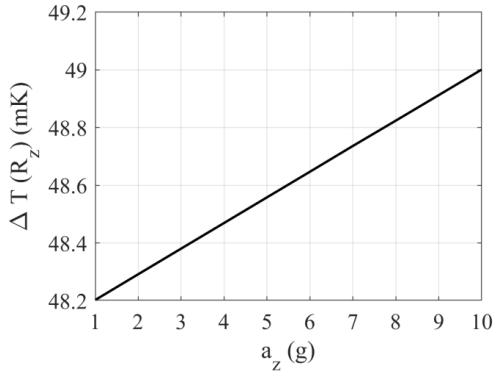

Fig. 6. The temperature difference $\Delta T(R_z) = \Delta T(R_{+z}) - \Delta T(R_{-z})$ at thermistors as a function of the acceleration component a_z, where $a_x = 0g$, $a_Y = 0g$, and the input heat power is equal to 3.1 mW.

IV. Summary and Conclusions

Thus, this paper presents a numerical model of the MEMS-based three-axis thermal accelerometer with proposed design, on the basis of which an analysis of possible ways to optimize its performance for detecting acceleration in three directions was carried out. This issue can be solved by using a set of thermoresistive sensing elements that are separated at different distances from the heater, which also allows you to choose their optimal position. The asymmetrical arrangement of the thermistors along the corresponding axis serves to increase the sensitivity for detecting accelerations in the range from 1g to 10g, respectively. The results obtained can be also applied to evaluate the performance of a multi-axis accelerometer with a given design. Further improvement of the proposed three-axis accelerometer model can be associated with modification of the geometry of the membrane and cavity within the existing technological capabilities to enhance the out-of-plane sensitivity, and with the implementation of this study on the detection of variable acceleration components at a given frequency.

Acknowledgment

The work was performed using the equipment of MIET Core Facilities Center «MEMSEC» and supported by the Ministry of Education and Science of RF (contract No. 14.581.21.0021, RFMEFI58117X0021).

References

[1] A. Kumar, A.O. Salau, S. Gupta and K. Paliwal, "Recent trends in IoT and its requisition with IoT built eningeering: a review," Advances in Signal Processing and Communication, in Select Proceedings of ICSC 2018, vol. 526, B. Rawat, A. Trivedi, S. Manhas and V. Karwal, Eds. Springer Singapore, pp. 15-25, 2018.

[2] H. Liu, K. Wei, Z. Li, W. Huang, Y. Xu and W. Cui, "A novel, hybrid-integrated, high-precision, vacuum microelectronic accelerometer with nano-field emission tips," Micromachines, vol. 9, p. 481, 2018.

[3] J.P. Lynch, A. Partidge, K. H. Law, T. W. Kenny, A.S. Kiremidjian and E. Carryer, "Design of piezoresistive MEMS-based accelerometer for integration with wireless sensing unit for structural monitoring," J. Aerosp. Eng., vol. 16, pp. 108-114, 2003.

[4] A. Aydemir, Y. Terzioglu and T. Akin, "A new design and a fabrication approach to realize a high performance three axes capacitive MEMS accelerometer," Sensors and Actuators A: Physical, vol. 244, pp. 324-333, 2016.

[5] T. Dinh, H.-P. Phan, A. Qamar, P. Woodfield, N.-T. Nguyen and D.V. Dao, "Thermoresistive effect for advanced thermal sensors: fundamentals, design considerations, and applications," J. Microelectromech. Syst., vol. 26(5), pp. 966-986, 2017.

[6] C.S. Silva, R.A. Dias, J.C. Viana, A.J. Pontes and L.A. Rocha, "Static and dynamic modelling of a 3-axis thermal accelerometer," Proc. Eng., vol. 47, pp. 973-976, 2012.

[7] X.B. Luo, Y.J. Yang, F. Zheng and Z.Y. Guo, "An optimized micromachined convective accelerometer with no proof mass," J. Micromech. Microeng., vol. 11, pp. 504-508, 2001.

[8] A. Garraud, A. Giani, P. Combette, B. Charlot and M. Richard, "A dual axis CMOS micromachined convective thermal accelerometer," Sensors and Actuators A: Physical, vol. 170(1-2), pp. 44-50, 2011.

[9] M. Han, J.K. Kim, S.H. Kong, S.-W. Kang and D. Jung, "Effect of heater geometry and cavity volume on the sensitivity of a thermal convection-based tilt sensor," Jpn. J. Appl. Phys., vol. 57, p. 06HJ01, 2018.

[10] K.E. Kaplan, M.M. Winterkorn, C.L.M. Everhart, D.D. Shin, G.J.O' Brien, F.B. Prinz and T.W. Kenny, "Active temperature compensation of thermal accelerometer for improved stability," Proceedings to the

2018 IEEE International Symposium of Inerial Sensors and Systems (INERTIAL), Moltrasio, Italy, March 26-29, 2018.

[11] L. Jiang, Y. Cai, H. Liu and Y. Zhao, "A micromachined monolithic 3 axis accelerometer based on convection heat transfer," Proceedings to the the 8th Annual IEEE International Conference on Nano/Micro Engineered and Molecular Systems, Suzhou, China, April 7-10, 2013.

[12] F. Mailly, H.B. Nguyen, L. Latorre and P. Nouet, "CMOS implementation of a 3-axis thermal convective accelerometer," Proceedings to the the 2014 IEEE Sensors Conference, Valencia, Spain, November 2-5, 2014.

[13] R. Mukherjee, J. Basu, P. Mandal and P.K. Guha, "A review of micromachined thermal accelerometers," J. Micromech. Microeng., vol. 27, p. 123002, 2017.

[14] J.K. Kim, M. Han, S.-W. Kang, S.H. Kong and D. Jung, "Multi-axis response of a thermal convection-based accelerometer," Micromachines, vol. 9, p. 329, 2018.

[15] H.B. Nguyen, F Mailly, L. Latorre and P. Nouet, "A new monolithic 3‐axis thermal convective accelerometer: principle, design, fabrication and characterization," Microsyst. Technol., vol. 21(9), pp. 1867-1877, 2015.

[16] Y. Ogami, N. Murakita and K. Fukudome, "Computational experiments on the step and frequency responses of a three-axis thermal accelerometer," Sensors, vol17, p. 2618, 2017.

[17] COMSOL Multiphysics® v. 5.4, website, www.comsol.com., COMSOL AB, Stockholm, Sweden.

[18] N.A. Djuzhev, D.V. Novikov, G.D. Demin, A.I. Ovodov and V.T. Ryabov, "An experimental study on MEMS-based gas flow sensor for wide range flow measurements," Proceedings to the the 2018 IEEE Sensors Applications Symposium (SAS), Seoul, South Korea, March 12-14, 2018.

[19] J. Fraden, "Velocity and acceleration," in Handbook of Modern Sensors, J. Fraden, Eds. Springer, Cham, pp. 379-411, 2016.